Jurnal Teknologi

Full Paper

MODELLING AND INTEGRATING OF EXPERIMENTAL ANALYSIS FOR PREDICTING THE PARAMETERS OF KENAF FIBRE-REINFORCED CONCRETE BEAM-COLUMN JOINT

Ige Samuel Ayeni[a,b]*, Yatim Mohamad Jamaludin[a], Nor Hasanah Abdul Shukor Lim[a]

[a]Faculty of Civil Engineering, Universiti Teknologi Malaysia, 81310 UTM Johor Bahru, Johor, Malaysia
[b]Department of Civil Engineering, The Federal Polytechnic, Ado-Ekiti, Nigeria

Article history
Received
10 August 2023
Received in revised form
4 September 2023
Accepted
23 September 2023
Published Online
18 February 2024

*Corresponding author
ayeni_is@fedpolyado.edu.ng

Graphical abstract

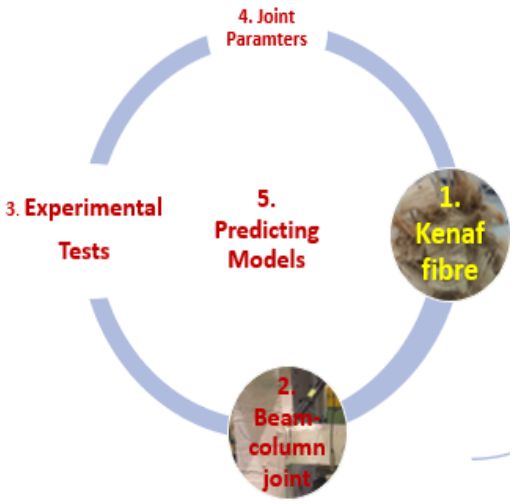

Abstract

To lessen the environmental impact of infrastructure projects, the construction sector has recently demonstrated a growing interest in sustainable materials. Kenaf fibre-reinforced concrete (KFRC), which has considerable mechanical qualities and biodegradability, has emerged as a possible eco-friendly substitute. The intricate interactions between material composition, geometrical factors, and load-bearing capacities make it difficult to optimise the design of structural parameters of KFRC beam-column joints. The beam column joints used in this study were designed based on ACI 318-19 shear criteria. This study suggests a novel method for precisely predicting the parameters of kenaf fibre-reinforced concrete beam-column (KFRC-BC) joints by combining machine learning modelling and experimental investigation. Experimental data were carefully documented to establish the reality, including load-displacement responses and beam-column joint parameters such as shear, stiffness, ductility, crack load, energy absorption, and ultimate load. These data were used in the modelling through GeneXproTools 5.0 and an empirical relationship with mathematical expressions has been proposed for each joint parameter. R2 statistical analysis is used to evaluate the model's efficacy. Deep learning could predict precisely concrete structure parameters. The shear spacing could be increased by 25% to 50%. Concrete strength influences all these characteristics. Kenaf fibre increased joint shear load, load at first crack, stiffness, ductility, ultimate load, and energy absorption by 4.89% to 28.5%, 10.12% to 34.1%, 6.65% to 10.74%, 14.71% to 52.06%, 10.52% to 25%, and 10% to 50.99%, respectively. These findings show that machine learning has clarified performance in the prediction aspect and proposed high accuracy of joint parameters.

Keywords: Beam, Column, Models, Joint, Parameters, Kenaf, Fibre, GeneXprotools 5.0

Abstrak

Untuk mengurangkan kesan alam sekitar projek infrastruktur, sektor pembinaan baru-baru ini menunjukkan minat yang semakin meningkat terhadap bahan mampan. Konkrit bertetulang gentian Kenaf (KFRC), yang mempunyai kualiti mekanikal yang besar dan kebolehbiodegradan, telah muncul sebagai pengganti mesra alam yang mungkin. Interaksi yang rumit antara komposisi

bahan, faktor geometri dan kapasiti galas beban menjadikannya sukar untuk dioptimumkan. Reka bentuk parameter struktur sambungan rasuk-lajur KFRC. Sambungan tiang rasuk yang digunakan dalam kajian ini direka bentuk berdasarkan kriteria ricih ACI 318-19. Kajian ini mencadangkan kaedah baru untuk meramalkan parameter sambungan rasuk konkrit bertetulang gentian kenaf (KFRC-BC) dengan tepat dengan menggabungkan pemodelan pembelajaran mesin dan penyiasatan eksperimen. Data eksperimen telah didokumenkan dengan teliti untuk mewujudkan realiti, termasuk tindak balas anjakan beban dan parameter sambungan rasuk-lajur seperti ricih, kekakuan, kemuluran, beban retak, penyerapan tenaga, dan beban muktamad. Data ini digunakan dalam pemodelan melalui GeneXproTools 5.0 dan hubungan empirikal dengan ungkapan matematik telah dicadangkan untuk setiap parameter bersama. Analisis statistik R2 digunakan untuk menilai keberkesanan model. Pembelajaran mendalam boleh meramalkan parameter struktur konkrit dengan tepat. Jarak ricih boleh ditingkatkan sebanyak 25% hingga 50%. Kekuatan konkrit mempengaruhi semua ciri ini. Gentian Kenaf meningkatkan beban ricih sendi, beban pada retak pertama, kekakuan, kemuluran, beban muktamad, dan penyerapan tenaga sebanyak 4.89% kepada 28.5%, 10.12% kepada 34.1%, 6.65% kepada 10.74%, 14.71% kepada 52.06%, 14.71% kepada 52.06%, 25%, dan 10% hingga 50.99%, masing-masing. Penemuan ini menunjukkan bahawa pembelajaran mesin telah menjelaskan prestasi dalam aspek ramalan dan mencadangkan ketepatan tinggi parameter bersama.

Kata kunci: Balok, kolom, model, sambungan, parameter, Kenaf, serat, GeneXprotools 5.0

1.0 INTRODUCTION

The joint is the area of the column within the deepest beam's depth and frames the column. There are three types of joints in a moment-resisting frame: inner, external, and corner. It is essential to deal with high energy dissipated at beam-column joints. As a result, the Beam-Column joints must be sufficiently ductile and properly anchored [1]. The primary purpose of the beam-column joint is to maintain structural integrity and to offer excellent protection against earthquake loads and other loads [2]. In current Reinforced Concrete (RC) constructions, the performance of beam-column joints is frequently characterised by a lack of ductility, a quick loss of strength, and a low capacity for releasing energy that could lead to joint failure, as shown in Figure 1a. To prevent rapid structural failure, the requirements for strength and ductility must be met in a structure's beam-column joints [3]. However, high ductility requirements for the modern design standard common for RC constructions require a high steel ratio for shear reinforcement, which results in a small stirrup spacing. Furthermore, high clear coverings between concrete and steel reinforcement are required by tight durability specifications. Due to the dense steel reinforcement, combining these two facts and the current design trend of small cross-sectional-sized structural components results in significant constructional issues. An inadequate gap makes placing and vibrating fresh concrete a particularly challenging process, which in turn leads to issues with concrete compacting in beam-column structures [4].

In beam-column joints of fibre-reinforced concrete (FRC), including steel fibres in the concrete mixture increases the concrete's ductility, toughness, and energy dissipation capacity. However, as the percentage of fibre grows, steel-fibre-reinforced concrete (SFRC) combinations experience issues like inefficiency, homogeneity, and conglomeration [4]. For hardened SFRC under direct tension, strain hardening behaviour is challenging to produce. Using SFRC in the joint region, extensive research on beam-column junctions has been done. SFRC increases flexural strength, shear strength, ductility, and energy dissipation capacity, according to the experiment's findings. Investigating the research findings also reveals that SFRC, despite reducing the transverse reinforcement in the joints, cannot stop the reinforcement from slipping and the joint core from being harmed at high drifts. The most sophisticated and best FRC, HPFRCC, exhibits strain-hardening behaviour in direct tension tests. Flexural yielding of the beam end, diagonal cracking and concrete crushing in the joint panel, bar bond slip, and bar elongation are possible processes for beam-column joint failure [5].

The performance of a beam-column joint could be measured through its ductility, stiffness, energy absorption, shear strength and ultimate load-carrying capacity. There are proposed models to predict joint shear strength [6]. Li *et al.* [7] used numerical analysis

and machine learning to propose a masonry large-scale wall piers shear capability model. A five-story, seven-bay brick wall was used to validate the suggested model. Regarding the overall load-deflection behaviour, satisfactory results were found compared to well-known techniques from the literature.

However, there are few or no models to predict joint ductility, stiffness, energy absorption, and ultimate load-carrying capacity. Meanwhile, these parameters are essential to the performance of the column joint. Therefore, this research aims to provide suitable models to predict the joint shear strength, ductility, stiffness, energy absorption, and ultimate load-carrying capacity, as well as the predicted values to experimental results to obtain their degree of accuracy. The predicted models were developed through genexprotool 5.0 using the experimental results. This study is significant because it has the potential to revolutionise the design and optimisation of KFRC structural components, allowing engineers to take advantage of eco-friendly materials' benefits while assuring exceptional structural performance. A powerful toolkit for quickly anticipating the behaviour of KFRC-BC joints under various conditions is provided by integrating experimental data and machine learning, which helps speed up the design process and save time and money. The objective of this study highlights the efficacy of machine learning modelling in conjunction with experimental analysis as a transformative methodology for predicting critical parameters in kenaf fibre-reinforced concrete beam-column joints. By pushing the boundaries of sustainable construction materials, this research paves the way for a greener and more resilient built environment.

Figure 1a Joint Failure

1.1 OVERVIEW OF GENE EXPRESSION PROGRAMMING

Gene pro-programming and gene algorithms have been extended by gene expression programming (GEP). The original version of GP, which uses the Darwinian selection principle to create a computer-based model to solve the problem, was created by Jone Koza in 1988., which has the benefit of handling complicated problems with a small database and no predetermined equations [8]. An expression tree that is encoded in the chromosomes contains the developed gene expression [9]. The Karva programming language and several other computer languages such as C, C++, Ada, Fortran, Go, Java, JavaScript, Octave, Pascal, Perl, PHP, Phyton, R, Visual Basic, VB.Net, VBA, and Matlab can also be used to express the GEP expression. Although, literature shows that the expression tree is the most used language [10]. Different parameters are added or removed to best fit the outcomes of the experiment to create the GEP expression. In situations where analytical formulations are unavailable, empirical expressions can be produced using GEP [11]. One or more genes with a head and a tail can be present in the GEP expression. The terminal symbols for constants and variables in the gene's tail are 1, a, b, and c, but the terminal symbols for functions and mathematical operators are 1, a, b,, cos,*, and / in the gene's head [12]. A higher gene count typically leads to more complex functions. The running time has also increased because of the increase in chromosomes. Picking the fitness function, followed by picking the terminals and functions needed to form the chromosomes, is the typical simplified approach to establishing a new GEP model. The number of chromosomes, the head length, and the number of genes is next calculated. Finally, the linking functions and genetic operators are chosen. Figure 1b illustrates the methodical algorithmic flow of Gene Expression. Based on the experimental database, gene expression programming has developed into an effective tool for predicting the behaviour of structural elements in civil engineering applications. Researchers have utilised GEP to forecast the joint shear strength [11], high-performance concrete (HPC) mix compressive strength [8], crack width [10], compressive strength of RHA-mortal [12], compressive strength of recycle-aggregate concrete [13] and properties of sugarcane bagasse ash concrete [14].

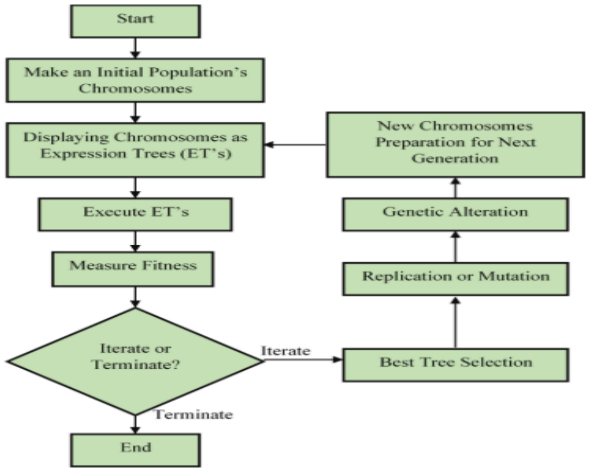

Figure 1b Methodical Algorithmic Flow of Gene Expression (Li *et al.*, 2022)

2.0 METHODOLOGY

The experiment used ASTM Type I cement from a single supplier. The coarse aggregate was made up of crushed granite with a maximum particle size of 10 mm. The fine aggregate utilised was river sand. With a wet and dry surface, the totals were batched. During the experiment, tap water was used for mixing and other duties. The Advanced Composite Research Laboratory, UTM, Malaysia acquired Kenaf fibre bast from Malaysia. Kenaf fibre bast was selected due to high content of cellulose that improves its engineering performance. To improve the adhesion between the fibres and the matrix and to remove hemicellulose, lignin, natural oil, and dirt from the fibre surface, the fibres were then subjected to a chemical treatment process that involved soaking them for three hours in 5% sodium hydroxide (NaOH). Decortications were followed by cleaning the fibres in distilled water until pH seven was reached, drying, brushing, and cutting into required lengths (Raviszi, 2017). According to earlier studies, the optimal kenaf fibre length and volume were 25 mm and 0.75%, respectively [17]. The main bar and shear reinforcement were made of high-yield steels with 16 mm and 8 mm diameters, respectively. The column and beam measured 1500x200x200 mm and 1000x150x150 mm, respectively, and were built in by ACI 318-19 shear criteria. The beam had 2Y16T and 2Y16B, while the column had 4Y16 for reinforcement. The beam was attached to the column at centre to form a joint. To ensure a weak beam in shear, the shear reinforcement spacings were increased by 0% (control), 25%, 50%, and 75% [18]. To study the influence of concrete strength on joint parameters, concrete grades 25 and 40 were designed using DOE method and used in this study. Tables 1 and 2 express the mix design proportion for both concrete grades. Rheobuild 1100GH was then used as a superplasticiser to enhance the workability of concrete [19]. During manufacturing, kenaf fibre was added to concrete to compensate for the lack of shear reinforcement. The impact of kenaf fibre on joint parameters was studied. In all, eight (8) samples of beam-column joints were prepared and tested. At 100mm from the end of the beam, the beam-column joint was loaded monotonously. LVDTs were installed at the joint to measure the joint deflection [20] as shown in Figure 2. The LVDT was connected to a load logger. Meanwhile, loads were applied by a hydraulic pump. Deflection and its corresponding load were recorded until the samples failed. Loads were plotted against deflection, and the slope of the curve gave stiffness. In contrast, the area under the curve gave energy absorption, and ductility was calculated by the ratio of ultimate deflection to deflection at yield [21]. Finally, joint shear load, joint load at first crack, and joint ultimate load were obtained [20]. The testing was done at the Structures and Materials Laboratory, Faculty of Civil Engineering, UTM, Malaysia.

2.1 Model Development

Gene expression programming is applied in this research using GeneXproTools 5.0 software to formulate joint shear strength, joint ultimate load carrying capacity, joint load at first crack, joint stiffness, joint ductility, and joint absorption energy models for exterior KFRC beam-column joint under monotonic loading. By altering the number of genes, chromosomes, head size, and linking function, many GEP models are created. The GEP model that was chosen best matched the outcomes of the experiment. Table 3 displays the chosen parameters for the GEP models that best fit the findings from the experiment.

Figure 2 Test Set-up

Table 1 Mix Fraction of Concrete Components (Grade 25)

Mix (MPa)	Slump (mm)	Cementitious (kg/m³)	10mm graded (kg/m³)	Sand (kg/m³)	Water (kg/m³)	W/C ratio	Fibre (kg/m³)	Super-plasticizer (ml/m³)
Plain concrete	60 - 180	431	887	777	250	0.58	-	149.6
Kenaf fiber concrete	60 - 180	427.77	880.35	771.17	248.13	0.47	17.58	148.45

Table 2 Mix Design of Kenaf Fibre-Reinforced Concrete (Grade 40)

Mix (MPa)	Slump (mm)	Cementitious (kg/m³)	10mm graded (kg/m³)	Sand (kg/m³)	Water (kg/m³)	W/C ratio	Fibre (kg/m³)	Superplasticizer (ml/m³)
Plain concrete	60 - 180	531.9	832.8	730.3	250	0.47	-	184.62
Kenaf fibre concrete	60 - 180	527.91	826.55	724.82	248.13	0.47	17.58	183.16

Table 3 Parameters for GEP model

S/N	GEP	
1	Functions: +, -, x-, /, exponential, natural log,	
2	Training: 6	
3	Validation: 2	
4	Number of Chromosomes: 30	
5	Head size: 7	
6	Number of genes:3	
7	Linking function: addition	
8	Constant per gene: 10	
8	Data type: floating	
9	Mutation rate: 0.00138	
10	Transposition rate: 0.00546	
11	Inversion rate: 0.00546	
12	One point recombination rate: 0.00277	
13	Two-point recombination rate: 0.00277	
14	Gene recombination rate: 0.00277	
15	Gene transportation rate: 0.00277	
Predictors	Lower limit	Upper limit
Shear Spacing	100mm	175mm
Concrete Grades	25	40
Response	Joint shear load, Joint Load at First Crack, Joint Stiffness, Joint Ductility, Joint Ultimate Load, and Joint Energy Absorption	

3.0 RESULTS AND DISCUSSION

This section focused on the results obtained from laboratory tests and predicted results derived using GeneXproTools 5.0.

3.1 Shear Strength, Load at First Crack and Ultimate Load

Table 4 expresses the load at first crack, shear, and ultimate loads obtained during testing of the eight (8) different beam-column joints. The load that caused first crack on the sample was taken as load at first crack while shear load was taken as load corresponding to shear crack (diagonal or inclined crack) during loading and ultimate load was measured as load at failure. These joints could be categorised into two (2) groups depending on their concrete grades. Comparing their performance in respect to their concrete grades, it is shown that joint with higher concrete grade performance better than lower concrete grade. This illustrated the contribution of compressive strength to joint performance in respect to load at first crack, shear load and ultimate load carrying capacity. For grades 25 and 40, the control joints had its first crack at load of 23.2 KN and 35.19 KN, respectively, while samples with higher shear spacing (125 mm and 150 mm) but with kenaf fibre as supplement gave 34.1% and 12.45%, 19.43% and 10.12% increment for grades 25 and 40, respectively. It should be submitted here that kenaf fibre impedes the crack formation in the beam-column joint, thereby improving the joint load at the first crack. Furthermore, both shear and ultimate loads were improved in joint samples with kenaf fibre. The contribution of kenaf fibre to prevent earliest possible occurrence of cracks (diagonal or straight) in beam-column joints ultimately increased the joint shear and ultimate loads. The fibre was able to bridge the gaps. For concrete grade 25, shear and ultimate loads improved by 28.5% and 15.9%, 25% and 18.75%, respectively while for concrete grade 40, shear and ultimate loads improved between 15.45% and 4.87%, 15.78% and 10.52%, respectively. In

addition, considering the effect of shear spacing and kenaf fibre on the studied joint parameters, the same Table shows that kenaf fibre could effectively enhanced all these parameters when the shear spacing is increased between 25% and 50%. Despite the shear deficiency, beam-column joints with kenaf fibre gave higher load at first crack, shear load, and ultimate load for all the concrete grades used. Fibres were found to significantly improve the joint's ability to tolerate shear cracks [22]. Hooda *et al*. [23] concluded that the introduction of fibres in concrete prevented the onset of cracks in fibre-reinforced concrete. On top of the aggregate bridging effect, concrete containing fibres offers a second bridging effect. Furthermore, fibres successfully bridged gaps from the micro to the macro scale, preventing cracks from spreading [24].

Table 4 Load at first Crack, Shear Load, and Ultimate Load

Concrete grades	Spacing (mm)	Load @ 1st crack (KN)	Load @ 1st shear crack (KN)	Load @ ultimate failure (KN)
25	100	23.2	28.8	51.2
25	125	31.19	37.01	64
25	150	26.09	33.40	60.8
25	175	22.11	25.45	57.6
40	100	35.19	44.92	60.8
40	125	42.03	51.84	70.4
40	150	38.75	47.11	67.2
40	175	32.67	37.55	64

3.1.1 Predicted Joint Load at First Crack

Figure 3 shows the model evidence from the software used. The software was able to select the best fitness for both testing and prediction. The relationship between the experimental and predicted is presented in Figure 4. This figure shows that both experimental and experiences declined at order 1 until they became improved at order 2. Also, both peak values at order three and three are equal at order 5. Finally, they ended up at a close margin at order 8 which was supported by their value of R^2 equal 0.94. The value of R^2 close to represents good closeness or agreement between the experimental and predicted model [25]. In addition, the model to predict the load corresponding to first crack was formulated by the addition of variables as presented by the software. This model is expressed in equation 1. The model is constrained by:

$$100 \leq d1 \leq 175$$
$$25 \leq d0 \leq 40$$

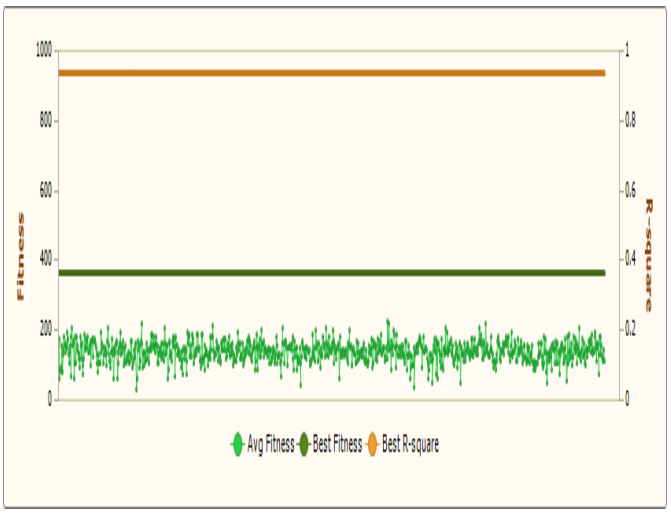

Figure 3 Model Evidence from The Software

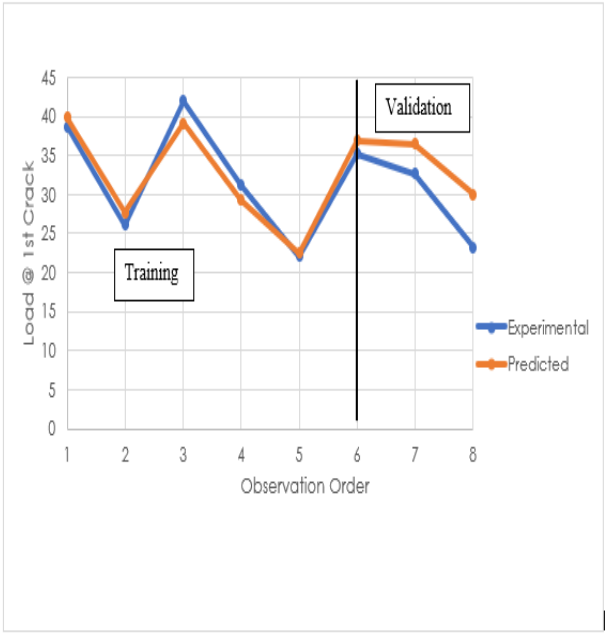

Figure 4 Experimental and predicted joint load at 1st crack

$$JLFC = 16.186 - \frac{2d1}{d0} + d0 - \frac{9.894d0}{d1} - \frac{d^2 0}{d1} + \log\{5.167\log d0 - 4.490 - \log d0\log d1 + 3.947\log d1\} \ldots\ldots\ldots\ldots\ldots\ldots\ldots\ldots\ldots\ldots\ldots\ldots (1)$$

where JLFC = Joint Load at first crack, d0 = concrete grade, d1 = shear spacing

3.1.2 Predicted Joint Shear Load

Figure 5 illustrated the behaviour of experimental and predicted shear load. It could be seen on the Figure that both had the same relationship with the observation orders. Their peak values were at order 2, while their lowest was at order 8. Their pattern of movement from order 1 to the last order was similar throughout the testing. The model for shear load was arrived at by adding the variables shown in expression tress in Figure 6. This model is shown in equation 2. The R^2 (0.96) shows that the model could predict the shear load with over 96% accuracy [10]. The model is constrained by:

$$100 \leq d1 \leq 175$$
$$25 \leq d0 \leq 40$$

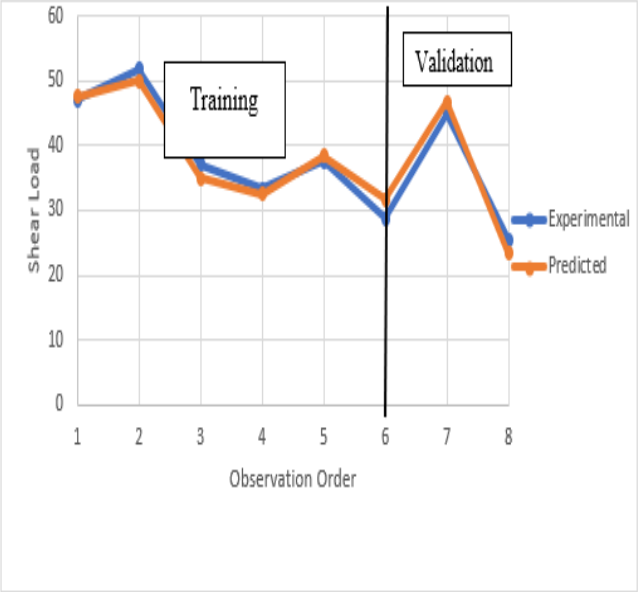

Figure 5 Experimental and predicted joint shear load

$$JSL = \frac{\left\{-0.3932d0 + \frac{106.3074d0}{d1} - 9.8064\right\}}{-0.3932 + 106.3074/d1} - \frac{3380.74}{d1} + 9.8119\log\{(0.2452d^2 1)(d1 - 26.586)\} \ldots\ldots\ldots\ldots\ldots\ldots\ldots\ldots\ldots\ldots\ldots\ldots (2)$$

where JSL = Joint Shear Load, d0 = concrete grade, d1 = shear spacing

3.1.3 Predicted Joint Ultimate Load

The experimental and predicted joint ultimate loads are expressed in Figure 6, with both having the same pattern during the testing. The model is expressed in Equation 3, which has about 83% accuracy (R^2 0.83). The model is constrained by:

$$100 \leq d1 \leq 175$$
$$25 \leq d0 \leq 40$$

Figure 6 Experimental and predited joint ultimate load

$$JUL = \left(\frac{(d0 * d0) * \log(G1C5)}{(G1C9 + d0) + G1C8}\right) + G2C6 - \left(\frac{(d1 + G2C9) * G2C0}{d1 - G2C9}\right)) + (((d0 + d1) + (d1 * G3C9))/((d1 * d0) - (G3C9 * d1))) \ldots\ldots\ldots\ldots\ldots\ldots\ldots\ldots\ldots\ldots\ldots\ldots (3)$$

where JUL = Joint Ultimate Load, d0 = concrete grade, d1 = shear spacing, G1C8 = −6.865720730000057, G1C5 = 4.017608836628997, G1C9 = −1.9820008048391 2, G2C6 = −4.4525420934845, G2C0 = 0.2528766403689 41, G2C9 = 95.84362518661 14, G3C9 = 23.26713965737 21

3.2 Experimental Joint Ductility

The ratio of ultimate deflection to deflection at yield is known as joint ductility. The ability of a material to tolerate plastic deformation without appreciably lowering its strength is referred to as ductility. Studies demonstrate that adding fibre to regular coarse aggregate enhances ductility. The percentage volume fraction added, however, has a considerable impact on its property [26]. Despite the lack of shear reinforcement, the volume percentage of kenaf fibre supplied at 0.75% significantly increased joint ductility, as indicated in Table 5. Joint ductility in joints with 125mm and 150mm shear spacing made of concrete grades 25 and 40 rose between 52.06% and 14.71%, 47.69% and 16.8%, respectively, compared to the control sample (100 mm shear spacing). The addition of Kenaf fibre increased joint ductility. When shear spacing was increased to 175 mm for both grades of concrete with the addition of kenaf fibre, this did not enhance joint ductility, which fell by 48.8% for grade 25 and 18.97% for grade 40. Meanwhile, it was reported that concrete is made more ductile when the fibre is introduced during manufacturing [27]. Also, the ductility of fibre-reinforced concrete was not affected when shear spacing was increased within a specific limit [23].

Table 5 Joint Ductility

Concrete grades	Spacing (mm)	Joint ductility
25	100	3.40
25	125	5.17
25	150	3.90
25	175	1.74
40	100	3.69
40	125	5.45
40	150	4.31
40	175	2.99

3.2.1 Predicted Joint Ductility

The experimental result of joint ductility was programmed into the GeneXproTools 5.0 software to get the predicted result. Figure 7 illustrates the sequence of experimental and predicted results. Both experienced declined patterns from orders 1 to 3. Also, from order 3 to 6, there was a corresponding increment for both results, then decreased values from order 6 to 7.5. This model is expressed in equation 4. The R^2 illustrates the degree of accuracy of the model equal to 0.9895. Although, the model is constrained by the following:

$$100 \leq d1 \leq 175$$
$$25 \leq d0 \leq 40$$

Figure 7 Experimental and predicted joint ductility

$$JD = \exp\left(\exp\left(\left(\frac{G1C4}{G1C6 - d1}\right) - (CG15 * d0)\right)\right) + \exp\left(\left(\frac{G2C0 * d0}{G2C8 - C3}\right)/\left((G2C3 * d0) - d1\right)\right) + \left(\left(\frac{d1}{G3C5}\right)/((d0 * d0) * \left(\frac{d0}{G3C6}\right)\right)) \quad \ldots\ldots\ldots\ldots\ldots\ldots\ldots\ldots (4)$$

where JD = Joint Ductility, $d0$ = concrete grade, $d1$ = shear spacing,

$G1C4 = -3.45241629790533, G1C6 = 2.59778695028535, G1C5 = -4.49419191428747, G2C0 = -0.386459568001699, G2C8 = 8.07796563615833,$

$G2C3 = 3.60717399305661, G3C6 = 8.75138004699851, \quad G3C5 = -9.5989867854854$

3.3 Experimental Joint Stiffness

The slope of the load-deflection curve is used to define the joint's relative stiffness. It decreased as more areas went to plastic hinges. Stiffness is the primary element influencing how effectively the joint functions. The stiffness of the various beam-column junctions under study is shown in Table 6. The stiffness of joints 125 mm and 150 mm for both grades of concrete rose between 7.44% and 3.33% for grade 25, 10.74% and 6.65% for grade 40. The specimen becomes stiffer when kenaf fibres are added. The stiffness of the joints improved while the shear spacing increased from 25% to 50%. To compensate for the lack of shear reinforcement, kenaf fibre might be used. Kenaf fibre was unable to make up for the insufficient shear reinforcement, which resulted in 39.7% and 38.36% decrease for grades 25 and 40, respectively, reduction in joint stiffness at a 75% increment shear spacing. The joint stiffness loss brought on by shear stress was reported that this shear stress could be minimised by avoiding the emergence of diagonal cracks and regional concrete crushing through the inclusion of fibre in concrete [28]. Compared to standard concrete specimens, the junction is stiffer with the addition of fibres [23].

Table 6 Joint Stiffness

Concrete grades	Spacing (mm)	Joint Stiffness
25	100	3.9
25	125	4.19
25	150	4.03
25	175	2.35
40	100	3.91
40	125	4.33
40	150	4.17
40	175	2.41

3.3.1 Predicted Joint Stiffness

The experimental joint stiffness result in Table 6 was used to predict joint stiffness. The result was divided into training and validation, as shown in Figure 8. The model generated is expressed in Equation 5. The R^2 (0.9647) value shown a strong agreement between the experimental and predicted results.

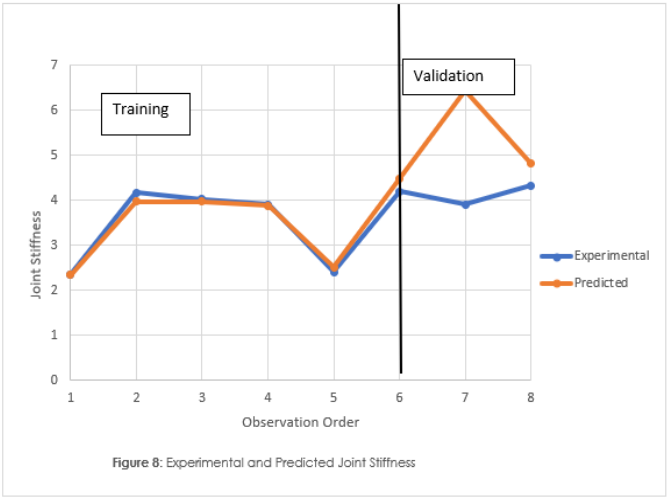

Figure 8 Experimental and predicted joint stiffness

$$JS = \left(\left(\frac{G1C5}{(d0+d1)-(d0*G1C3)}\right)+G1C6\right)+\left(\frac{(d1+d0)+(d0+d1)}{((G2C9+G2C6)+(d1-d0))}\right) + \left(\left(\frac{G3C3}{(d0-d1)+(d0*G3C1)}\right)+G3C2\right) \ldots\ldots\ldots\ldots\ldots\ldots\ldots (5)$$

where JS = Joint Stiffness, d0 = concret grade, d1 = shear spacing

G1C6 = 5.58312021240883, G1C5 = -7.3217871639149, G1C3 = 7.66845209730793, G2C9 = -6.77663502914518, G2C6 = -9.23719664725764, G3C2 = -5.46865760699231; G3C3 = -7.5294351023896; G3C1 = 3.51949634981323

3.4 Experimental Joint Energy Absorption

An illustration of the reinforced concrete beam's inelastic response is provided by toughness, another word for energy absorption capacity. It is calculated as the amount of energy absorbed per square inch of the cross-section of the reinforced concrete beam-column joint. The calculation of energy absorption capacity is based on the fracture mechanism of the reinforced concrete beam-column joint. Usually, it is estimated by taking an internal measurement of the load-deflection curve [29]. The results show that adding kenaf fibre significantly increases the reinforced concrete beam-column joint's capacity to absorb energy. This could be because of kenaf fibre's strong resistance to concrete's tensile cracking and ability to stop cracks efficiently. Energy absorption increased between 69.61% and 10% for joints with grade 25, 50.99% and 24.08% for joints with grade 40 compared to the control. There was a reduction in energy absorption when the shear spacing was increased to 175mm for both grades of concrete, as shown in Table 7. The kenaf fibre consistently restricts the crack opening at the reinforced concrete beam-column joint, leaving space for a large amount of energy to be absorbed. The equal distribution of kenaf fibre over the joint and effective crack-bridging activity of the fibres limit the lateral expansion of the reinforced concrete beam-column junction. Kenaf fibre-reinforced concrete is more resilient and can support higher loads during deflection because it prevents cracks from spreading.

Table 7 Energy Absorption

Concrete grades	Spacing (mm)	Joint Energy Absorption
25	100	358.47
25	125	608
25	150	394.29
25	175	301.33
40	100	533.12
40	125	805
40	150	661.5
40	175	419.4

3.4.1 Predicted Joint Energy Absorption

To predict the joint energy absorption, experimental data are needed. Therefore, the experimental result presented in Table 7 was used. The software was able to partition the data into training and validation. In both testing phases, experimental and predicted results behaved the same way. In order 8, a little gap exists between the experimental and predicted results, as shown in Figure 9. The R^2 value of 0.999 expresses a good relationship between experimental and predicted results. The model is illustrated in Equation 6

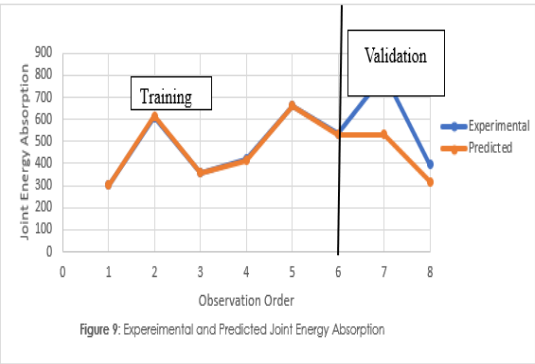

Figure 9: Expereimental and Predicted Joint Energy Absorption

Figure 9 Experimental and predicted joint energy absorption

$$JEA = \{\frac{\left(\frac{d1}{d0}\right)-(G1c9*d1)}{(G1c6-d1)+(d0*G1c5)}\}+(d1/((G2c2*(G2c4-d0))-(d0+d1))) + \{((d0-d1)-(d0*G3c6))+((G3c1*G3c5) * log d1))\} \ldots\ldots\ldots\ldots\ldots\ldots\ldots\ldots\ldots\ldots\ldots\ldots\ldots\ldots\ldots\ldots (6)$$

where JEA = Joint Energy Absorption, do = concrete grade, d1 = shear spacing, G1C9 = −6.22687027441452, G1C6 = −282.863077609033, G1C5 = 10.9578980901271, C2 = −9.75135385689312, G2C4 = 9.57073552659688, G3C6 = −9.56473650032313, G3C1 = −4.224110687228882, G3C5 = −10.1490305936295

4.0 CONCLUSION

In the current experiment, eight beam-column junctions with varied shear spacings were studied under a monotonically increasing load. To determine the effect of including kenaf fibres on the performance of joints, specimens (125, 150, and 175mm) with volume fractions of 0.75% kenaf fibres were cast and evaluated. The control sample specimens had 100mm shear spacing. The following joint parameters were experimentally determined and predicted using the selected software: shear load, load at first crack, joint stiffness, joint ductility, joint energy absorption, and ultimate joint load. All the parameters were enhanced by including kenaf fibre at shear spacing increments between 25% and 50% for all the grades of concrete used. Shear spacing, concrete grades, and kenaf fibre are

important components in the experimental section. It was discovered that kenaf fibre may compensate for a lack of shear reinforcement in beam-column joints. The joint shear load increased between 4.89% and 28.5%, the load at first crack improved between 10.12% and 34.1%, stiffness, ductility, ultimate load, and energy absorption. were found to increase between 6.65% and10.74%, 14.71% and 52.06%, 10.52% and 25%, and 10% and 50.99%, respectively compared to the control sample. The experimental and predicted models had a high level of agreement. R2 values ranging from 0.834 to 0.999 indicate a good relationship. Finally, GEP-derived mathematical equations are substantially simpler and are recommended for use in routine-based design practice. It is critical to note that the derived GEP equations are only valid within the input data range used during the formulation.

Conflicts of Interest

The author(s) declare(s) that there is no conflict of interest regarding the publication of this paper.

Acknowledgement

The Ministry of Higher Education, Fundamental Research Scheme, (Grant Nos. FRGS/1/2021/TK01/UTM/02/1andRJ130000.7851.5F426, Technicians, and Faculty of Civil Engineering, Universiti Teknologi Malaysia all provided funding for this study, which the authors sincerely thank.

References

[1] M. Rezvani Sharif and M. S. Ketabi. 2020. An Improved Plastic Hinge Relocation Technique for RC Beam–Column Joints: Experimental and Numerical Investigations. *Bulletin of Earthquake Engineering*. 18: 4191-4225. Doi: 10.1007/s10518-020-00855-7.

[2] A. Nagaraju and V. B. Reddy Suda. 2022. An Experimental Study on R.C Beam-Column Joints under Cyclic Loading. *Mater. Today Proc.* 52: 608-616. Doi: 10.1016/j.matpr.2021.10.043.

[3] C. E. Chalioris and K. E. Bantilas. 2017. Shear Strength of Reinforced Concrete Beam-Column Joints with Crossed Inclined Bars. *Eng. Struct.* 140: 241-255. Doi: 10.1016/j.engstruct.2017.02.072.

[4] M. H. Saghafi, A. Golafshar, M. S. Zareian, and A. H. Mehri. 2021. Application of HPFRCC in Beam–Column Joints to Reduce Transverse Reinforcements. *Structures*. 31(February): 805-814. Doi: 10.1016/j.istruc.2021.02.032.

[5] F. Ma, M. Deng, and Y. Yang. 2021. Experimental Study on Internal Precast Beam–Column Ultra-High-Performance Concrete Connection and Shear Capacity of Its Joint. *J. Build. Eng.* 44(May): 103204. Doi: 10.1016/j.jobe.2021.103204.

[6] I. Mansouri, E. M. Güneyisi, and K. M. Mosalam. 2021. Improved Shear Strength Model for Exterior Reinforced Concrete Beam-Column Joints Using Gene Expression Programming. *Eng. Struct.* 228(April): 111563. Doi: 10.1016/j.engstruct.2020.111563.

[7] H. Li, J. Li, and V. Farhangi. 2023. Determination of Piers Shear Capacity Using Numerical Analysis and Machine Learning for Generalization to Masonry Large Scale Walls. *Structures*. 49(January): 443-466. Doi: 10.1016/j.istruc.2023.01.095.

[8] F. Aslam *et al.* 2020. Applications of Gene Expression Programming for Estimating Compressive Strength of High-Strength Concrete. *Adv. Civ. Eng.* Doi: 10.1155/2020/8850535.

[9] H. S. Ullah, R. A. Khushnood, J. Ahmad, and F. Farooq, 2022. Predictive Modelling of Sustainable Lightweight Foamed Concrete using Machine Learning Novel Approach. *J. Build. Eng.* 56(March): 104746. Doi: 10.1016/j.jobe.2022.104746.

[10] F. Althoey *et al.* 2022. Machine Learning Based Computational Approach for Crack Width Detection of Self-Healing Concrete. *Case Stud. Constr. Mater.* 17(October): e01610. Doi: 10.1016/j.cscm.2022.e01610.

[11] Y. Murad. 2020. Joint Shear Strength Models for Exterior RC Beam-column Connections Exposed to Biaxial And Uniaxial Cyclic Loading. *J. Build. Eng.* 30(June): 101225. doi: 10.1016/j.jobe.2020.101225.

[12] M. A. Haque, B. Chen, M. F. Javed, and F. E. Jalal. 2022. Evaluating the Mechanical Strength Prediction Performances of Fly Ash-based MPC Mortar with Artificial Intelligence Approaches. *J. Clean. Prod.* 355(March): 131815. Doi: 10.1016/j.jclepro.2022.131815.

[13] V. Quan Tran, V. Quoc Dang, and L. Si Ho. 2022. Evaluating Compressive Strength of Concrete Made with Recycled Concrete Aggregates Using Machine Learning Approach. *Constr. Build. Mater.* 323(November): 126578. Doi: 10.1016/j.conbuildmat.2022.126578.

[14] M. I. Shah, M. F. Javed, F. Aslam, and H. Alabduljabbar. 2022. Machine Learning Modeling Integrating Experimental Analysis for Predicting The Properties of Sugarcane Bagasse Ash Concrete. *Constr. Build. Mater.* 314: 125634. Doi: 10.1016/j.conbuildmat.2021.125634.

[15] P. Li *et al.* 2022. Sustainable Use of Chemically Modified Tyre Rubber in Concrete: Machine Learning Based Novel Predictive Model. *Chem. Phys. Lett.* 793(February): 139478. Doi: 10.1016/j.cplett.2022.139478.

[16] M. Ravizi. 2017. Performance of Kenaf Fibre Reinforced Concrete Under. Thesis. Civil Eng. Fac. Civ. Eng. Univ. Teknol. Malaysia.

[17] L. T. Fook and J. M. Yatim. 2015. Mechanical Properties of Kenaf Fiber Reinforced Concrete with Different Fiber Content and Fiber Length. *J. Asian Concr. Fed.* September: 10-21. Doi: doi.org/10.18702/acf.2015.09.1.11.

[18] A. A. Abbas, S. M. Syed, and D. M. Cotsovos. 2014. Seismic Response of Steel Fibre Reinforced Concrete Beam – Column Joints. *Eng. Struct.* 59: 261-283. Doi: 10.1016/j.engstruct.2013.10.046.

[19] R. Ahmad, R. Hamid, and S. A. Osman. 2019. Effect of Fibre Treatment on the Physical and Mechanical Properties of Kenaf Fibre Reinforced Blended Cementitious Composites. *KSCE J. Civ. Eng.* 1-14. Doi: 10.1007/s12205-019-1535-7.

[20] A. Rajeev, S. S. Parsi, S. N. Raman, T. Ngo, and A. Shelke. 2020. Experimental and Numerical Investigation of an Exterior Reinforced Concrete Beam-Column Joint Subjected to Shock Loading. *Int. J. Impact Eng.* 137(January): 103473. Doi: 10.1016/j.ijimpeng.2019.103473.

[21] N. Ganesan, P. V. Indira, and M. V. Sabeena. 2014. Behaviour of Hybrid Fibre Reinforced Concrete Beam-Column Joints Under Reverse Cyclic Loads. *Mater. Des.* 54: 686-693. Doi: 10.1016/j.matdes.2013.08.076.

[22] F. Ma, M. Deng, and Y. Yang. 2021. Experimental Study on Internal Precast Beam–column Ultra-high-performance Concrete Connection and Shear Capacity of Its Joint. *J. Build. Eng.* 44(May): 103204. Doi: 10.1016/j.jobe.2021.103204.

[23] N. Hooda, J. Narwal, B. Singh, V. Verma, and P. Singh. 2013. An Experimental Investigation on Structural Behaviour of Beam Column Joint. *Int. J. Innov. Technol. Explor. Eng.* 3: 84.

[24] M. Khan, M. Cao, and M. Ali. 2020. Cracking Behaviour and Constitutive Modelling of Hybrid Fibre Reinforced Concrete. *J. Build. Eng.* 30(February): 101272. Doi: 10.1016/j.jobe.2020.101272.

[25] S. H. Park, D. Yoon, S. Kim, and Z. W. Geem. 2021. Deep Neural Network Applied to Joint Shear Strength for Exterior RC Beam-column Joints Affected by Cyclic Loadings. *Structures*. 33(May):1819-1832. Doi: 10.1016/j.istruc.2021.05.031.

[26] P. Manibalan, G. Abirami, R. Baskar, and N. Pannirselvam. 2023. Ductile Behavior of Reinforced Concrete Beam Incorporated with Basalt Fiber. *Innov. Infrastruct. Solut.* 8(1). Doi: 10.1007/s41062-023-01033-9.

[27] P. Pooja, V. Girija, K. Vidhya, M. J. Carmichael, B. Nithya, and M. P. Sureshkumar. 2021. Beam-Column Joint: Structural Sehaviour Using Hybrid Fibres. *Mater. Today Proc.* Doi: 10.1016/j.matpr.2021.07.192.

[28] F. Hanif and T. Kanakubo. 2017. Shear Performance of Fiber-reinforced Cementitious Composites Beam-column Joint Using Various Fibers. *J. Civ. Eng. Forum*. 3(2): 383. Doi: 10.22146/jcef.26571.

[29] A. I. Rather, A. R. Dar, and A. F. Ghowsi. 2020. Improved Performance of Steel Fibre Reinforced Beam-Column Joint - An Experimental Study. *Mater. Today Proc.* 32: 982-988. Doi: 10.1016/j.matpr.2020.05.674.